



Compressed learning for real-time ECG signals classification

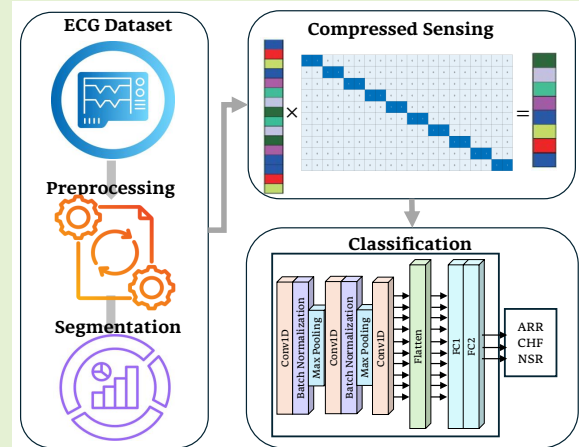
Title	Compressed learning for real-time ECG signals classification
Author(s)	Lal, Bharat;Abolghasemi, Vahid;Gravina, Raffaele;O'Keeffe, Derek;Roshan, Davood
Publication Date	2026-02-06
Publisher	Institute of Electrical and Electronics Engineers
Repository DOI	https://doi.org/10.1109/JSEN.2026.3660078

Compressed Learning for Real-Time ECG Signals Classification

Bharat Lal, Vahid Abolghasemi, Raffaele Gravina, Derek O’Keeffe, and Davood Roshan *Senior Members, IEEE*

Abstract— Electrocardiograms (ECGs) are essential for diagnosing cardiac conditions, yet high-fidelity 12-lead signals pose challenges for storage, transmission, and real-time processing. Compressed Sensing (CS) addresses these issues by exploiting signal sparsity, but its reliance on complex reconstruction algorithms limits practical deployment. Compressed Learning (CL) offers a more efficient alternative by enabling direct feature extraction from compressed measurements. This paper proposes an optimized CL framework for classifying arrhythmia (ARR), congestive heart failure (CHF), and normal sinus rhythm (NSR) from compressed ECG signals. We introduce a deterministic block-sparse binary sensing matrix with diagonal block allocation of ones and zeros elsewhere. This lightweight design eliminates floating-point multiplications, reduces memory overhead, and ensures uniform computational complexity across compression ratios. Compared with widely used Gaussian, Bernoulli, and Fourier sensing matrices, the proposed approach preserves ECG morphology more effectively and is well suited for embedded hardware. A deep learning-based Convolutional Neural Network (CNN) is developed and benchmarked against conventional machine learning classifiers, demonstrating superior classification accuracy across all tested compression ratios redachieving up to 96.56% accuracy, 96.5% F1-score, and 97.9% specificity at CR = 0.5, and outperforming Gaussian and Bernoulli matrices. To validate real-time feasibility, the proposed matrix is implemented on an STM32 NUCLEO-F401RE microcontroller. Hardware experiments confirm that the framework achieves high accuracy while significantly reducing energy consumption and computational load requiring only 9 μ s per compression operation and consuming 0.641 μ J with constant-time execution across CRs. Furthermore, the proposed framework is validated on three widely used PhysioNet databases (MIT-BIH Arrhythmia, Normal Sinus Rhythm, and BIDMC Congestive Heart Failure), which together capture diverse patient populations and varying acquisition devices. This ensures robustness of the method and supporting its applicability in diverse clinical environments. Extending this framework to wearable ECG systems represents a promising direction for future research.

Index Terms— Compressed Sensing, Compressed Learning, ECG Classification, Compressed Measurements, Machine Learning (ML)



This project has received funding from the European Union’s Horizon Europe Excellent Science programme under the Marie Skłodowska-Curie Actions Grant Agreement [Grant Agreement No 101081457] and in part from CÚRAM, Research Ireland Centre for Medical Devices [under Grant Reference 13/RC/2073.P2. We acknowledge co-funding from Next Generation EU, in the context of the National Recovery and Resilience Plan, Project SERICS “Security and rights in the cyberspace” (PE00000014). The views and opinions expressed are only those of the authors and do not necessarily reflect those of the European Union or the European Commission. Neither the European Union nor the European Commission can be held responsible for them.

(*Corresponding Author: Bharat Lal, bharat.lal@universityofgalway.ie) Bharat Lal and Derek O’Keeffe are with CÚRAM, Research Ireland Centre for Medical Devices, University of Galway, Ireland. Raffaele Gravina is with the Department of Informatics, Modeling, Electronics and Systems Engineering, University of Calabria, Rende (CS) 87036, Italy. Vahid Abolghasemi is with the School of Computer Science and Electronic Engineering (CSEE), University of Essex, CO4 3SQ, UK. Davood Roshan is with the School of Mathematical and Statistical Sciences, CÚRAM, Research Ireland Centre for Medical Devices, University of Galway, Ireland

I. INTRODUCTION

ELECTROCARDIOGRAM signals are among the most widely used physiological signals in healthcare, playing a vital role in assessing heart health and detecting potential abnormalities. For clinicians and researchers, such signals offer invaluable insights into cardiac function, making them crucial tools for diagnosing a range of conditions, from arrhythmias to heart failure. However, continuous monitoring of ECG signals poses significant challenges in data storage, transmission, and processing where efficient real-time analysis is crucial, especially in resource-limited settings.

Traditionally, ECG signals are sampled at high rates, following the Nyquist-Shannon theorem to capture all necessary details. While effective, this approach generates large volumes of data that demand substantial storage and computational resources. In response to these challenges, researchers have

turned to compressed sensing as an innovative solution [1]. CS utilizes the inherent sparsity of ECG signals, allowing for accurate reconstruction from a compressed measurement [2]. This process significantly reduces data size while preserving the critical diagnostic information required for clinical assessments. Despite its potential, CS often involves complex and computationally intensive reconstruction steps, which can be impractical for real-time applications. This limitation has led to the development of compressed learning (CL) approach that bypasses full reconstruction [3], [4]. Instead, CL enables the direct extraction of features from compressed measurements. Recent studies [5]–[8] have shown that compressed learning can be highly effective for ECG analysis, demonstrating strong results in detecting abnormalities such as atrial fibrillation (AF) using machine learning models trained directly on compressed data.

However, despite recent advances in CL, several challenges remain unresolved, particularly in the design of structured sparse sensing matrices that achieve high compression with minimal information loss. One major limitation of current CL frameworks is their reliance on either random or learnable sensing matrices, which often suffer from poor hardware compatibility or increased training complexity [9]. Furthermore, traditional machine learning models struggle to extract discriminative features directly from compressed data, due to their limited capacity for hierarchical representation learning. To address these limitations, this paper introduces an optimized compressed learning framework that integrates a fixed, structured, sparse binary block diagonal sensing matrix with a lightweight Convolutional Neural Network (CNN). The proposed method enables efficient ECG signal classification by learning directly from compressed measurements, eliminating the need for costly reconstruction. The framework is specifically designed to identify clinically relevant ARR, CHF, and NSR signals with high accuracy and low computational overhead. Additionally, the proposed matrix is implemented and validated on a low-power microcontroller to demonstrate its feasibility in real-time scenarios.

The key contributions of this paper are summarized as follows:

- We design a structured sparse binary sensing matrix optimized for real-time ECG compression, offering consistent computational efficiency across compression ratios. The matrix requires no multiplications and maintains constant-time complexity.
- We propose a lightweight CNN that learns discriminative features directly from compressed ECG signals. The model achieves 96.56% accuracy, 96.5% F1-score, and 97.9% specificity at CR = 0.5.
- We compare the proposed method against Gaussian, Bernoulli, and Fourier sensing matrices and multiple ML classifiers, demonstrating superior performance. The method improves accuracy by 10–13% over random matrices at low CRs.
- We implement the sensing matrix on an STM32 NUCLEO-F401RE microcontroller. The hardware achieves 9 μ s latency and 0.641 μ J energy consumption, confirming suitability for wearable devices.

This paper is organized as follows: Section II reviews related work and outlines the motivation for this study. Section III presents the preliminaries of compressed learning for ECG signals. Section IV details the proposed methodology. Section V presents the experimental results and comparisons with existing methods. Section VI discusses the key findings, hardware implementation, limitations, and potential directions for future research. Finally, Section VII concludes the paper and outlines future research directions.

II. RELATED WORK AND MOTIVATION

A. Background and Related Work

Numerous studies have investigated CS for ECG applications, aiming to enhance compression and reconstruction quality. For example, Zhang et al. [10] introduced the Block Sparse Bayesian Learning (BSBL) algorithm, utilizing spatial and temporal structures to compress and reconstruct fetal ECG signals effectively. Izadi et al. [11] applied the Kronecker technique and adaptive dictionary learning to improve reconstruction, while Abhishek et al. [12] developed a biorthogonal wavelet based on double-sided exponential splines, achieving superior reconstruction quality. Other notable approaches include two-dimensional mapping for improved sparsity [13], incorporation of prior support information [14], and low-rank constraints that exploit spatial and temporal ECG signal structures [15]. Additionally, Saliga et al. [16] utilized a dynamic ECG model to reduce noise interference, while Rezaii et al. [17] proposed a method to optimize sparsity for noise robustness. Despite the advantages of traditional CS, some limitations persist in practical applications. For instance, the measurement matrix often lacks structural information from the original signal, which can lead to reduced reconstruction quality, particularly at low sensing rates. Moreover, issues related to matrix storage, computational demands, and reconstruction speed hinder CS adoption. These limitations make CS methods impractical for deployment on power-constrained devices.

With advancements in deep learning, CS has expanded into data-driven methods that enhance performance by learning signal characteristics directly from data. Deep neural networks, such as Convolutional Neural Networks (CNNs), replace traditional measurement matrices with learnable layers, enabling end-to-end optimization without requiring signals to be sparse. This adaptability has led to a range of deep learning-based CS applications [18], [19]. For instance, Muduli et al. [20] introduced a Stacked Denoising Autoencoder (SDAE) to compress and reconstruct fetal ECG signals, while Polania et al. [19] employed Restricted Boltzmann Machines (RBMs) to capture ECG sparsity patterns, thereby enhancing accuracy. Mangia et al. [21] proposed a CNN with short windows to reduce computation complexity. Other methods include CNN-based CS frameworks for EEG signals [22], oracle-based decoders [23], and multi-layer perceptron networks trained with stochastic gradient descent [24]. Compared to traditional CS, deep learning-based methods exploit inter-data relationships to achieve higher reconstruction accuracy. Traditional systems require full reconstruction (or decompression) of

the original signal before diagnosis by humans or machines. However, learnable sensing matrices and deep decoders often require high memory and computation, limiting deployment on embedded hardware.

The reconstruction step in CS remains computationally expensive, often prohibiting its use in real-time scenarios. CL addresses this limitation by directly extracting features from compressed measurements, thus bypassing the reconstruction step and reducing computational complexity [25], [26]. Moreover, extracted features can be used for tasks like arrhythmia detection, heart rate classification, or abnormality detection without needing the full ECG signals. In this regard, several studies have contributed to the application of CS and CL for ECG signal processing. For instance, Da Poian *et al.* [27] proposed Compressed Sensing Matched Filtering (CSMF) for detecting R-peaks in compressed ECG data, which enables the extraction of RR intervals without full signal reconstruction. Building on the concept of CL, Zhang *et al.* [28] introduced a simple deterministic measurement matrix (SDMM) and a Transposed Projection-Convolutional Neural Network (TP-CNN) to enhance AF detection in wearable devices, achieving high accuracy with reduced power consumption. Similarly, Siddique *et al.* [29] explored the use of low-power approximate adders in digital CS for Internet of Things (IoT) healthcare systems, illustrating that critical event detection in biomedical signals can be achieved with energy efficiency. Yet, majority of CL approaches still rely on random or semi-structured matrices that may not consistently preserve ECG morphology, especially at low compression ratios.

Further advancements in compressed ECG analysis include the use of specific machine learning models. Abdelazez *et al.* [25] employed Random Forest on compressed ECG data to detect AF using discrete cosine transform, statistical methods, and wavelet transforms. This approach demonstrated reliable AF detection, affirming the feasibility of machine learning in compressed signal classification. Additionally, a study by Laudato *et al.* [30] introduced a method for heart rate estimation by identifying R-peaks in a single-lead ECG using a circulant sensing matrix and random forest classifier, contributing valuable insights into low-resource, high-efficiency classification methods for compressed data. Another study by Zhang *et al.* [31] utilized a 1-D Convolutional Neural Network for feature extraction directly from compressed ECG signals, further underscoring the potential of deep learning in the CL domain. However, many of these methods focus on specific arrhythmias or limited datasets, reducing their generalizability across broader ECG conditions.

Some studies have explored the potential of structured and learned matrices to optimize compressed measurements. For example, the Structured Fourier Matrix (SFM) has shown promise for faster acquisition and lower storage requirements compared to traditional random Gaussian matrices [32]. Meanwhile, Kumar *et al.* [33] reviewed the importance of choosing the correct measurement matrix, particularly highlighting the advantages of structured matrices and the benefits of learned matrices, such as neural network-based approaches, in providing adaptive and effective compression. Nonetheless, many structured or learned matrices still rely on floating-point

operations or retraining, which can limit their suitability for resource-constrained wearable ECG systems.

B. Motivation

The existing literature on compressed learning methods either depend on unstructured random sensing matrices or trainable deep encoders. While effective in theory, these approaches suffer from hardware inefficiency, unpredictable performance, and increased training complexity. Additionally, traditional machine learning classifiers applied to compressed data often lack the capacity to learn discriminative features, particularly when signal fidelity is degraded due to aggressive compression. This research is motivated by the need to bridge these gaps through a deterministic and hardware-friendly compressed learning solution. Specifically, we aim to develop a structured sparse binary sensing matrix that eliminates the reconstruction step while preserving essential diagnostic features. When combined with a lightweight CNN classifier, this approach enables direct, real-time ECG classification from compressed measurements, achieving a balance between classification accuracy and energy efficiency.

III. PRELIMINARIES

Compressed sensing also known as compressive sensing or sampling fundamentally differs from conventional undersampling. While undersampling deterministically discards time-domain samples and may introduce aliasing and irreversible information loss, compressed sensing acquires signals through linear projections that preserve global signal information under sparsity and incoherence assumptions. Compressed learning further extends the concept of compressed sensing by allowing direct feature extraction from compressed data. Mathematically, the compressed ECG signal y can be represented as:

$$y = \Phi x \quad (1)$$

where $x \in \mathbb{R}^{N \times 1}$ is the original ECG signal, $\Phi \in \mathbb{R}^{M \times N}$ ($M \ll N$) is the measurement matrix, and $y \in \mathbb{R}^{M \times 1}$ is the compressed signal. Traditional CS approaches require the reconstruction of x from y , which can be computationally intensive [34]. In contrast, CL methods bypass reconstruction, directly extracting features from y for classification purposes.

The choice of measurement matrix Φ is crucial in CL, as it determines the quality of compressed measurements and the accuracy of feature extraction. In this paper, we propose a sparse binary sensing matrix and compare the performance with various state-of-the-art sensing matrices at different compression ratios (CRs). The CR quantifies the reduction in data size achieved during compression. It is defined as:

$$\text{CR} = \frac{M}{N} \quad (2)$$

where M is the size of the compressed data, and N is the original data size. In our study, we evaluate a range of CRs from 0.1 to 0.9 to investigate how varying levels of compression impact classification accuracy, aiming to strike a balance between efficient data compression and reliable classification performance.

Once the compressed ECG measurements are obtained, we employ a CNN-based deep learning model trained directly on the compressed measurements. Furthermore, Section IV-C provides a detailed description of the compressed learning process for ECG signal classification, in which feature extraction is performed directly on the compressed data, eliminating the need for signal reconstruction. Additionally, we compare the classification performance of the proposed approach with state-of-the-art machine learning classifiers.

IV. METHODS AND MATERIALS

This section outlines the methodology and materials utilized in this study to develop and evaluate a CL framework for ECG signal classification. The proposed framework integrates block sparse binary sensing matrices along with a classification model. Additionally, we describe the datasets used in the study, along with the performance evaluation metrics, applied to assess the effectiveness of model across different settings.

A. Dataset

In this study, we utilize three publicly accessible ECG datasets from PhysioNet: the BIDMC Congestive Heart Failure, the MIT-BIH Normal Sinus Rhythm, and the MIT-BIH Arrhythmia. Each of these databases was originally sampled at different frequencies, so to maintain consistency across our classification tasks, we adjust the sampling rates where necessary. Table I shows a summary of the specifications of these datasets. What follows provides further details on each dataset separately.

1) *MIT-BIH Normal Sinus Rhythm Database*: The MIT-BIH Normal Sinus Rhythm Database [35] includes 18 long-term ECG recordings from healthy individuals without significant arrhythmias. This dataset, sampled natively at 128 Hz, contains recordings from 5 men (aged 26 to 45) and 13 women (aged 20 to 50). As indicated in Table I, we allocate 15 records (80%) for training and 3 records (20%) for testing. This dataset provides a baseline for normal cardiac rhythms and enables the model to distinguish between healthy and pathological signals.

2) *BIDMC Congestive Heart Failure Database*: The BIDMC Congestive Heart Failure Database [36] contains long-term ECG recordings from 15 individuals diagnosed with severe congestive heart failure (NYHA class 3–4), including 11 men (aged 22 to 71) and 4 women (aged 54 to 63). Each recording spans approximately 20 hours, recorded over two ECG channels at an original sampling frequency of 250 Hz. For this study, we downsample these signals to 128 Hz, ensuring compatibility with the other datasets. As shown in Table I, 12 records (80%) were selected for training, and the remaining 3 records (20%) were used for testing.

3) *MIT-BIH Arrhythmia Database*: The MIT-BIH Arrhythmia Database [35], [37], a widely used dataset in arrhythmia research, contains 48 half-hour ECG recordings from 47 individuals (25 men aged 32 to 89 years, and 22 women aged 23 to 89 years), sampled at 360 Hz. This dataset captures a variety of arrhythmic events, making it invaluable for arrhythmia detection. To align with the other datasets, we downsample this database to 128 Hz. Out of 47 records, we use 39 (80%) for training and 9 (20%) for testing, as summarized in Table I.

TABLE I: Dataset Training and Testing Set Distribution

Dataset: BIDMC Congestive Heart Failure (Total Records: 15)	
Training Set (80%)	Testing Set (20%)
chf01, chf02, chf03, chf04, chf05, chf06, chf07, chf08, chf09, chf10, chf11, chf12	chf13, chf14, chf15
Dataset: MIT-BIH Normal Sinus Rhythm (Total Records: 18)	
Training Set (80%)	Testing Set (20%)
16265, 16272, 16273, 16420, 16483, 16539, 16773, 16786, 16795, 17052, 17453, 18177, 18184, 19088, 19090	19093, 19140, 19830
Dataset: MIT-BIH Arrhythmia Database (Total Records: 47)	
Training Set (80%)	Testing Set (20%)
100, 101, 102, 103, 104, 105, 106, 107, 108, 109, 111, 112, 113, 114, 115, 116, 117, 118, 119, 121, 122, 123, 124, 200, 201, 202, 203, 205, 207, 208, 209, 210, 212, 213, 214, 215, 217, 219, 220	221, 222, 223, 228, 230, 231, 232, 233, 234

B. Design of the Sensing Matrix

Design of the sensing matrix Φ is the most important task in compressed sensing/learning. Random sensing matrices (e.g., Gaussian, Bernoulli) are widely used because they are, with high probability, incoherent with any sparsifying basis and satisfy the Restricted Isometry Property (RIP), ensuring accurate recovery or feature preservation. Although their universality makes them an attractive choice, random sensing matrices are hardware-inefficient and computationally demanding [9], [38]. This has motivated researchers to either optimize the sensing process or design application-specific structured matrices, which are particularly advantageous in CL, where full signal reconstruction is not always required. Here, we propose a structured sparse binary block sensing matrix, as shown in the Algorithm 1 where features deterministic block allocations of ones along the diagonal and zeros elsewhere. This innovate approach eliminates the need for floating-point operations and significantly reducing memory and processing demands. Figure 1 illustrates representative samples of the proposed matrix at CR = 0.4 to 0.7. As observed, the matrix structure maintains consistent sparsity while adapting the block size to the compression level (e.g., Block Size = 2 for CR = 0.5, and mixed sizes for CR = 0.6), ensuring uniform computational complexity across CRs. Although the RIP is central in compressed sensing for ensuring accurate signal reconstruction [2], it is not a strict requirement in compressed learning since no reconstruction is performed [6], [39]. Instead, the key requirement is that the compressed measurements retain class-discriminative features. The deterministic block allocation in the proposed matrix lowers inter-column coherence and preserves local continuity of ECG morphology, thereby enabling stable feature extraction in the compressed domain. These structural properties provide a theoretical rationale for the consistent classification performance observed across compression ratios.

C. End-to-End Framework Overview

The complete CL-based ECG classification pipeline is shown in Fig 2. It consists of three main stages: (a) data acquisition, preprocessing, and segmentation, (b) compression via the proposed sensing matrix, and (c) classification using a custom-designed CNN.

Algorithm 1 Generation of Binary Block Sensing Matrix

Require: Signal dimension N , Number of compressed measurements M

Ensure: Binary Sensing Matrix $\Phi \in \{0, 1\}^{M \times N}$

- 1: Initialize an empty sensing matrix: $\Phi \leftarrow \mathbf{0}_{M \times N}$
- 2: Compute base block size: $b \leftarrow \lfloor N/M \rfloor$
- 3: Compute remaining columns: $r \leftarrow N - (b \times M)$
- 4: Initialize starting column index: $c_{\text{start}} \leftarrow 1$
- 5: **for** $i = 1$ **to** M **do** \triangleright Iterate over rows to construct the matrix
- 6: **if** $r > 0$ **then**
- 7: Assign block size: $b_i \leftarrow b + 1$ \triangleright Distribute extra columns
- 8: Update remaining columns: $r \leftarrow r - 1$
- 9: **else**
- 10: Assign block size: $b_i \leftarrow b$
- 11: **end if**
- 12: Compute column end index: $c_{\text{end}} \leftarrow \min(c_{\text{start}} + b_i - 1, N)$
- 13: Assign ones in the sensing matrix: $\Phi(i, c_{\text{start}} : c_{\text{end}}) \leftarrow 1$
- 14: Update column start index: $c_{\text{start}} \leftarrow c_{\text{end}} + 1$
- 15: **end for**
- 16: **return** Φ

1) *Data Acquisition and Segmentation:* ECG recordings from three clinical conditions, i.e., ARR, CHF, and NSR, are extracted from benchmark PhysioNet datasets (Table I). Each signal is resampled to 128 Hz, denoised, normalized, and then segmented into uniform lengths. For this study, various uniform segment sizes (128, 256, 512, 1024, and 2048 samples) were tested, with the segment size of 128 yielding the best performance in terms of classification accuracy and computational efficiency. Through this empirical evaluation, a segment length of 128 samples was selected for optimal performance.

2) *Compression Stage:* Each segment is independently compressed using the proposed $\Phi_{M \times N}$ matrix. Due to its binary and structured layout, the compression operation involves only addition and indexing operations and ideal for hardware-efficient implementation on embedded IoT devices.

3) *CNN-Based Classification Model:* The compressed vector y is directly fed into a 1D CNN designed to learn features in the compressed domain. The model consists of stacked Conv1D layers with batch normalization and max pooling, followed by fully connected layers for final classification into ARR, CHF, or NSR. This architecture is lightweight yet capable of extracting rich hierarchical features directly from compressed inputs. Table II outlines the model architecture used at CR = 0.5. The CNN was trained using categorical cross-entropy as the loss function and optimized with the Adam optimizer (learning rate = 0.0005). Training was performed for up to 100 epochs with a batch size of 256, applying early stopping with a patience of 15 epochs to prevent overfitting and restore the best model weights. The architecture included dropout layers (rate = 0.4) after each

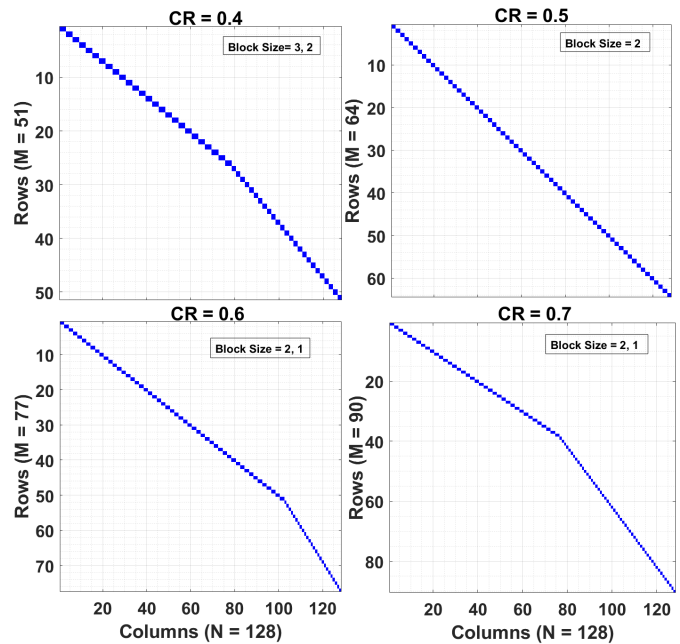


Fig. 1: Proposed Sensing Matrix sample at CR= 0.4, 0.5, 0.6 and 0.7

fully connected layer, along with L2 weight regularization to enhance generalization. The performance was evaluated using 5-fold classwise stratified cross-validation

TABLE II: Proposed CNN Architecture at CR = 0.5

Layer	Kernel	Filters	Output Shape	Parameters
Conv1D	2	64	(64, 64)	192
MaxPooling1D	-	-	(32, 64)	0
BatchNorm	-	-	(32, 64)	256
Conv1D	2	128	(32, 128)	16,512
MaxPooling1D	-	-	(16, 128)	0
BatchNorm	-	-	(16, 128)	512
Conv1D	1	256	(16, 256)	33,024
Flatten	-	-	4096	0
Dense (FC1)	-	-	128	524,416
Dense (FC2)	-	-	64	8,256
Dense (Softmax)	-	-	3	195

D. Benchmark Comparisons

To validate the generalization and robustness of the proposed CL framework, we conducted extensive comparisons using both alternative sensing matrices and a broad set of traditional machine learning classifiers. First, we evaluated three widely used sensing matrices Random Gaussian Matrix (RGM), Random Bernoulli Matrix (RBM), and Structured Fourier Matrix (SFM) and compared their performance with the proposed block-sparse binary matrix across all compression ratios. The results show that the proposed matrix consistently achieves superior classification accuracy, specificity, and F1-score. Second, we benchmarked the proposed CNN against a comprehensive suite of classical and ensemble learning methods, each trained on the same original and compressed ECG measurements.

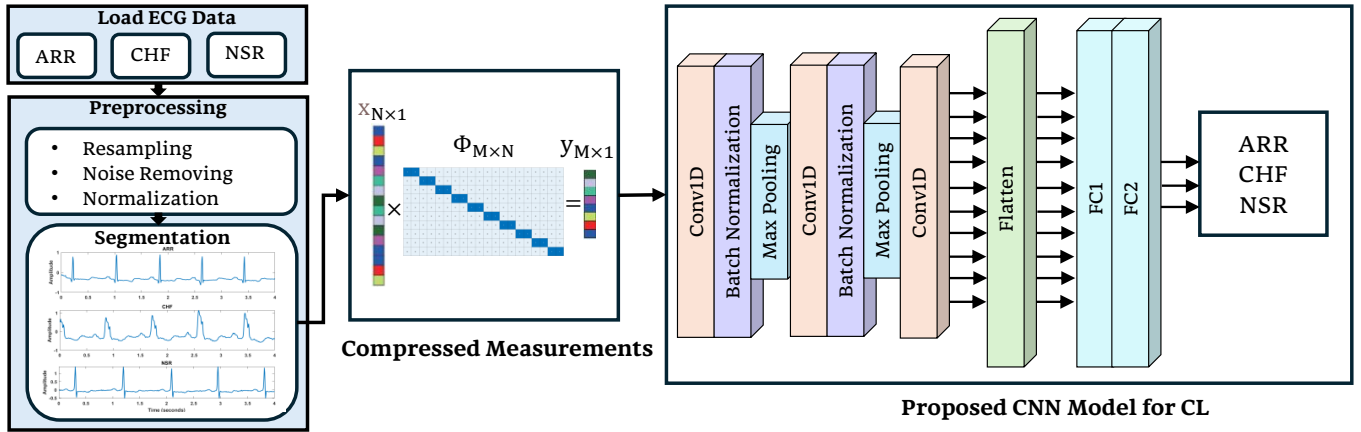


Fig. 2: Proposed compressed learning pipeline with sparse sensing matrix and CNN classifier

E. Performance Evaluation Metrics

We employ a range of performance metrics to provide a view of the proposed sensing matrix and model performance. Including accuracy, precision, recall, specificity, F1-score, and computational efficiency. Each metric provides unique insights into different aspects.

$$\text{Accuracy} = \frac{TP + TN}{TP + TN + FP + FN} \quad (3)$$

Accuracy is the proportion of correctly classified samples out of the total samples. Accuracy gives us an overall measure of how well the model performs across all classes.

$$\text{Precision} = \frac{TP}{TP + FP} \quad (4)$$

Precision or positive predictive value, represents the proportion of true positive predictions out of all positive predictions. High precision indicates that the model is reliable in its positive classifications, reducing false positives.

$$\text{Recall} = \frac{TP}{TP + FN} \quad (5)$$

Recall, also known as sensitivity, measures the model's ability to identify all true instances of a particular class. High recall minimizes false negatives, which is specifically important in medical applications where missed detections can have serious implications.

$$\text{Specificity} = \frac{TN}{TN + FP} \quad (6)$$

Specificity, or true negative rate, quantifies the model's ability to correctly identify negative cases. It is crucial in contexts where false positives can lead to unnecessary follow-up actions or treatments, thus providing a complementary perspective to recall.

$$\text{F1-Score} = 2 \times \frac{\text{Precision} \times \text{Recall}}{\text{Precision} + \text{Recall}} \quad (7)$$

F1-Score is the harmonic mean of precision and recall, providing a balanced metric that accounts for both false positives and false negatives. It is especially valuable when dealing with

imbalanced datasets, as it gives a single metric reflecting both the model's precision and recall.

In the above equations, TP is true positives, TN is true negatives, FP is false positives, and FN is false negatives, representing the classification outcomes.

V. RESULTS

To evaluate the performance of the proposed CL framework, we systematically analyzed ECG classification across compression ratios ranging from 0.1 to 0.9. At each CR, the original ECG signals were compressed using the proposed sparse binary sensing matrix and subsequently classified using the proposed CNN model. The classification performance was assessed using 5-fold cross-validation, with the results summarized in Table III and visualized in Fig. 3. As evident from the results, classification performance improves progressively with increasing CR up to 0.5. Specifically, accuracy increases from 90.12% at CR = 0.1 to 96.56% at CR = 0.5, accompanied by a similar rise in F1-score, precision, and recall. This performance gain is attributed to the increasing number of compressed measurements and improved preservation of signal information. Notably, at CR = 0.5, the sensing matrix exhibits a perfectly structured block diagonal pattern with a uniform block size of 2, which ensures optimal coverage and minimal overlap between sensing elements. This structure appears to be particularly conducive to both signal preservation and learning efficiency in the CNN model.

Interestingly, a minor dip in performance is observed at CR = 0.6 (accuracy = 96.14%), despite an increase in the number of compressed measurements. This anomaly can be attributed to the structural change in the sensing matrix at CR = 0.6, where the block configuration deviates from a uniform design. As shown in Fig. 1, the block size alternates between 2 and 1 to complete the diagonal coverage, introducing irregularity in measurement uniformity and potentially affecting signal representation quality. Nevertheless, performance recovers and stabilizes beyond CR = 0.7, culminating in the highest recorded accuracy of 96.73% at CR = 0.9.

Among all metrics, specificity demonstrates a uniquely consistent upward trend across compression levels from 93.80%

at CR = 0.1 to 97.90% at CR = 0.5 and 97.99% at CR = 0.9. This improvement reflects the increasing capacity of the model to correctly identify true negative cases (i.e., healthy or non-event signals), which is particularly critical in clinical applications where minimizing false positives is essential to avoid unnecessary interventions or alarms.

Additionally, the standard deviation values across all metrics show a decreasing trend with higher CRs, highlighting enhanced model stability and reduced variance in predictions. For example, the standard deviation of accuracy drops significantly from $4.94 (\times 10^{-3})$ at CR = 0.2 to just $1.83 (\times 10^{-3})$ at CR = 0.9. Similar reductions are observed in F1-score, precision, recall, and specificity. This behavior further supports the robustness of the proposed approach under more densely measured and structurally consistent compression. Both structural analysis of the sensing matrices and statistical evaluation of classification outcomes shows the effectiveness of the proposed framework.

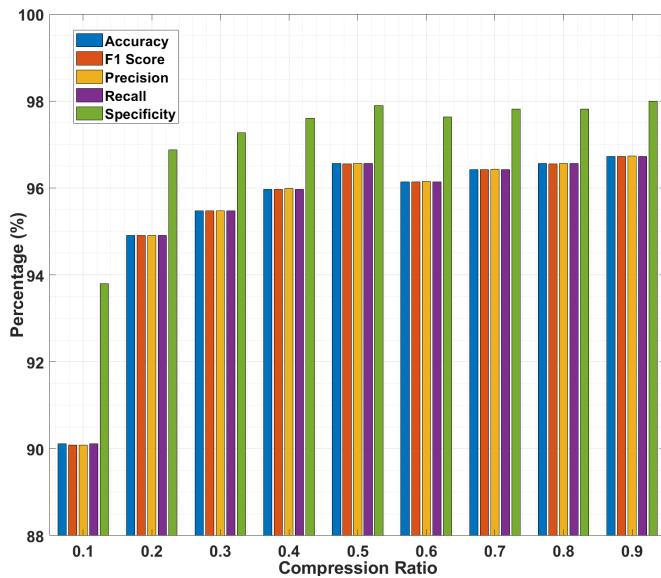


Fig. 3: Trends of Accuracy, F1-Score, Precision, Recall, and Specificity across compression ratios.

TABLE III: Average ECG classification performance at different compression ratios using 5-fold cross-validation

CR (%)	Accuracy (%)	Std ($\times 10^{-3}$)	F1 Score (%)	Std ($\times 10^{-3}$)	Precision (%)	Std ($\times 10^{-3}$)	Recall (%)	Std ($\times 10^{-3}$)	Specificity (%)	Std ($\times 10^{-3}$)
0.1	90.116	3.515	90.084	3.599	90.088	3.597	90.116	3.515	93.800	2.647
0.2	94.908	4.940	94.904	4.931	94.910	4.898	94.908	4.940	96.878	2.625
0.3	95.476	2.660	95.474	2.636	95.478	2.601	95.476	2.660	97.266	1.272
0.4	95.972	3.698	95.972	3.661	95.984	3.573	95.972	3.698	97.602	1.408
0.5	96.562	4.064	96.556	4.090	96.568	4.025	96.562	4.064	97.900	2.439
0.6	96.144	3.159	96.140	3.146	96.152	3.093	96.144	3.159	97.638	2.312
0.7	96.424	1.515	96.424	1.492	96.434	1.442	96.424	1.515	97.812	1.209
0.8	96.562	2.034	96.554	2.040	96.560	1.995	96.562	2.034	97.820	1.988
0.9	96.726	1.826	96.726	1.826	96.734	1.758	96.726	1.826	97.994	1.171

A. Performance Comparison with Different Sensing Matrices

To verify the effectiveness of the proposed sensing matrix, we compare its performance against three commonly adopted sensing strategies: RGM, RBM, and SFM, across a range of compression ratios from 0.1 to 0.9. The evaluation considers

three key metrics: accuracy, F1 score, and specificity. The results are tabulated in Table IV. Statistical significance was also assessed using paired bootstrap resampling across folds, with superscripts in Table IV indicating differences relative to the proposed method that are significant at the 1% level.

From the comparison, it clearly shows that the proposed method consistently outperforms all baseline sensing matrices across all compression ratios. For instance, at a low compression ratio of 0.1, the proposed approach achieves an accuracy of 90.12%, whereas RGM, RBM and SFM yield 77.19%, 77.40% and 68.864%, respectively. This margin of improvement (over 13% than RGM and RBM) highlights the superior signal retention properties of the proposed sensing matrix even under CR=0.1.

As the compression ratio increases, the performance of the baseline methods also improves gradually, but they still lag significantly behind the proposed method. At CR = 0.5, the proposed matrix yields an accuracy of 96.56%, compared to 85.75% (RGM), 85.89% (RBM), and 88.23% (SFM). The gap persists across all higher CRs, with the proposed method maintaining accuracy levels above 96%. The superiority of the proposed approach is not only evident in accuracy but also in F1-score and specificity. High F1-scores of proposed method (e.g., 96.726% at CR = 0.9) indicate balanced sensitivity and precision, confirming the model reliability in both detecting and correctly classifying abnormal heartbeats. Moreover, specificity values remain consistently high, reaching 97.994% at CR = 0.9 outperforming the best baseline (SFM at 94.186%) by a significant margin. Since the proposed binary block sampling matrix does not heavily randomize the data samples, the key features of the ECG signals are well preserved after compression. As a result, significantly higher classification accuracy is achieved. This highlights a key advantage of the proposed framework: it prioritizes feature encoding alongside compression, rather than focusing on signal reconstruction.

B. Performance Comparison with State-of-the-Art ML Classifiers

To provide a comprehensive evaluation of the proposed compressed learning framework, we benchmarked its performance against a wide range of classical and ensemble machine learning classifiers. All models were evaluated using 5-fold cross-validation on the original ECG segments (128 samples) as well as on the compressed measurements produced by four different sensing matrices: the RGM, RBM, SFM, and the proposed block-diagonal sparse binary sensing matrix. For each matrix, ECG signals were compressed at three representative compression ratios, CR = 0.1, 0.5, and 0.9, enabling a balanced assessment across low, medium, and high compression levels. Importantly, the same compressed measurements were used for all classifiers without any additional preprocessing or reconstruction, ensuring fair comparisons across methods and compression conditions.

Table V presents the 5-fold cross-validation accuracy results, while Table VII lists the hyperparameters of the baseline models. These results show clear differences in how various classifiers respond to different sensing matrices. For uncompressed ECG signals and those compressed using random

TABLE IV: Classification performance of different sensing matrices across various compression ratios using 5-fold cross-validation. Reported values are the averages across folds. Superscripts (***) denotes statistically significant differences compared to the Proposed method at the 99% confidence level, based on paired bootstrap resampling across folds.

Compression Ratio		0.1	0.2	0.3	0.4	0.5	0.6	0.7	0.8	0.9
RGM	Accuracy (%)	77.194***	83.030***	86.158***	86.164***	85.752***	86.516***	86.018***	86.600***	86.652***
	F1 Score (%)	76.940***	82.880***	86.076***	86.074***	85.642***	86.438***	85.918***	86.450***	86.558***
	Specificity (%)	85.590***	89.218***	91.298***	91.302***	91.048***	91.598***	91.246***	91.480***	91.668***
RBM	Accuracy (%)	77.404***	82.210***	84.705***	85.836***	85.886***	85.866***	86.784***	86.788***	86.776***
	F1 Score (%)	76.992***	81.920***	84.565***	85.758***	85.760***	85.772***	86.708***	86.675***	86.744***
	Specificity (%)	85.582***	88.566***	90.245***	91.196***	91.136***	91.258***	91.808***	91.710***	92.060***
SFM	Accuracy (%)	68.864***	84.466***	82.486***	79.728***	88.226***	85.238***	81.758***	89.374***	90.470***
	F1 Score (%)	65.886***	84.456***	82.500***	79.282***	88.202***	85.218***	81.446***	89.390***	90.458***
	Specificity (%)	77.744***	90.732***	89.536***	86.592***	92.868***	91.038***	88.126***	93.720***	94.186***
Proposed	Accuracy (%)	90.116	94.908	95.476	95.972	96.562	96.144	96.424	96.562	96.726
	F1 Score (%)	90.084	94.904	95.474	95.972	96.556	96.140	96.424	96.554	96.726
	Specificity (%)	93.800	96.878	97.266	97.602	97.900	97.638	97.812	97.820	97.994

matrices (RGM and RBM), the Fine KNN and Weighted KNN models deliver the highest accuracy. These random matrices tend to preserve pairwise distances between samples, thereby maintaining the local neighbourhood structure that KNN classifiers rely on. However, these matrices also incur higher memory usage and computational overhead, making them less suitable for real-time or resource-constrained embedded applications. Consequently, the primary aim of this research is to develop a lightweight sensing matrix tailored for real-time deployment. When the ECG signals were compressed using structured matrices (SFM or the proposed block-sparse binary matrix), the performance characteristics changed significantly. Classical models such as discriminant analysis, decision trees, SVM variants, and neural networks are less accurate as compression increases, reflecting their limited ability to extract discriminative features from structured compressed domains. In contrast, the proposed CNN demonstrates strong and consistent performance when trained directly on compressed measurements. For example, the proposed sensing matrix with CNN achieves accuracies of 90.12% at CR = 0.1, 96.56% at CR = 0.5, and 96.72% at CR = 0.9, outperforming all classical and ensemble learning models under the same conditions.

C. Comparison with State-of-the-art studies

To comprehensively validate the effectiveness of our proposed method, we compare it against a wide range of state-of-the-art methods reported in the literature. The comparative analysis considers multiple aspects, including the use and type of compressed sensing, reconstruction strategy, classifier architecture, compression ratio, and key evaluation metrics such as accuracy, specificity, and F1-score. The results are summarized in Table VI.

Among the compared studies, several do not implement CS (e.g., [40], [41], and [42]), instead relying on traditional transforms such as Discrete Cosine Transform (DCT), Continuous Wavelet Transform (CWT), or segment-level classification using raw ECG data. While these methods report high accuracy (up to 98.7% in [41]), their lack of data compression restricts their applicability in real-time or resource-constrained

environments such as wearable devices or edge computing systems.

Other studies that incorporate CS use a variety of sensing matrices. For instance, [43] employs deep compressed sensing, which although effective, introduces higher computational complexity due to the learnable matrix requiring gradient updates during training. Similarly, [44] uses a learnable sensing matrix within CSML-Net, achieving accuracies up to 98.13% but at the cost of architectural complexity and hardware implementation challenges.

The study in [45] uses an optimized Walsh-Hadamard matrix and explores multiple combinations of raw, compressed, and reconstructed ECG signals with CNNs. Their best reported accuracy (95.0%) using raw ECG is slightly lower than ours, despite more complex processing and the use of SPGL1 for reconstruction. Notably, signal reconstruction used in many of these studies adds latency and computational overhead, making them less suitable for real-time systems.

Several works, including [31] and [46], employ random or semi-structured sensing matrices such as Random Gaussian Matrix (RGM), Random Sparse Matrix, or Sparse Binary Matrix (SBM). These unstructured or weakly structured matrices lack the deterministic measurement allocation present in our proposed binary block sparse matrix, resulting in either reduced accuracy (e.g., 94.46% in [31]) or inconsistency across CRs.

Our method utilizes a deterministic sparse binary block diagonal sensing matrix, which offers a favorable trade-off between complexity and performance. It avoids the need for reconstruction and achieves strong classification results directly from compressed measurements, reducing processing latency and computational cost. At compression ratios of 0.5, 0.6, and 0.7, our framework achieves accuracies of 96.56%, 96.14%, and 96.42%, respectively placing it among the top performers in the reconstruction free field. Additionally, specificity values of up to 97.9% and F1-scores exceeding 96% demonstrate the model's excellent reliability and robustness, especially in minimizing false positives a critical consideration in clinical ECG analysis.

Compared to works such as [44] and [43], our approach reduces training overhead by employing a fixed structured

TABLE V: 5-fold Cross Validation Accuracy (%) for Original Signal and Compressed (CR = 0.1, 0.5, 0.9) ECG Classification

Classifier Name	Original Signal 128 samples	CR = 0.1				CR = 0.5				CR = 0.9			
		RGM	RBM	SFM	Proposed	RGM	RBM	SFM	Proposed	RGM	RBM	SFM	Proposed
Gaussian Naive Bayes	39.97	46.38	47.30	58.16	47.161	41.85	41.82	62.31	40.718	40.86	41.01	61.59	40.126
Kernel Naive Bayes	39.97	46.38	47.30	58.16	58.322	41.85	41.82	62.31	56.443	40.86	41.01	61.59	56.083
Linear Discriminant	58.98	58.89	58.88	59.26	58.885	58.88	58.88	58.92	58.879	58.90	58.91	58.90	58.958
Quadratic Discriminant	66.31	58.68	60.55	48.23	52.138	62.09	62.10	65.71	61.499	65.49	65.68	50.22	66.496
Coarse Tree	59.26	59.26	59.26	59.26	59.259	59.26	59.26	66.55	59.751	59.26	59.26	66.55	59.783
Medium Tree	63.06	59.51	59.54	61.17	63.634	61.11	59.80	68.45	64.643	60.97	60.36	68.41	64.414
Fine Tree	68.21	63.35	61.63	62.38	68.486	64.70	64.17	74.99	68.082	65.06	65.45	75.08	68.406
Efficient Logistic Regression	58.33	58.45	58.64	59.26	56.999	58.33	58.33	58.34	57.013	58.32	58.33	58.34	57.585
Efficient Linear SVM	59.01	59.00	59.04	59.26	59.259	58.98	58.97	58.99	59.259	58.99	58.99	58.99	53.202
Narrow Neural Network	75.15	66.59	63.79	63.48	72.608	74.79	74.67	82.44	75.315	75.30	75.40	82.34	75.654
Medium Neural Network	80.72	69.42	67.50	64.42	76.315	80.45	80.61	85.06	81.389	81.24	80.83	85.29	81.622
Bilayer Neural Network	77.91	68.28	65.60	63.84	74.891	77.60	77.92	83.14	77.231	77.90	78.01	83.25	77.987
Trilayer Neural Network	78.12	69.04	66.78	63.55	75.559	78.24	78.42	83.53	78.092	78.85	78.42	84.37	77.851
Wide Neural Network	87.31	74.58	72.52	65.21	81.712	86.16	86.25	87.88	87.18	86.99	87.27	88.20	87.171
Boosted Tree Ensemble	70.66	64.57	61.20	62.34	68.167	68.51	67.44	80.43	68.083	69.40	69.08	80.81	68.202
Kernel Logistic Regression	59.26	60.67	59.45	58.69	70.805	59.26	59.26	59.26	76.347	59.26	59.26	59.26	79.816
Bagged Trees Ensemble	88.29	77.36	75.26	66.06	85.076	84.43	83.54	86.13	86.241	85.16	84.44	86.44	87.362
RUSBoosted Trees Ensemble	60.18	52.84	46.05	37.46	56.814	56.98	56.03	75.66	55.77	57.72	56.99	75.70	55.91
Coarse Gaussian SVM	55.96	24.86	24.52	20.56	60.513	46.58	45.78	40.00	61.214	54.19	53.64	52.16	61.658
Kernel SVM	41.86	55.94	54.90	51.05	70.043	44.06	43.63	43.03	76.076	42.70	42.83	43.14	80.492
Coarse KNN	77.58	73.95	70.89	60.87	78.796	77.27	76.55	65.07	77.144	77.05	76.74	62.99	77.687
Medium KNN	88.05	81.74	80.04	64.49	86.465	87.54	87.66	75.88	87.946	87.90	88.00	74.88	87.902
Weighted KNN	89.67	83.21	81.87	65.54	87.748	89.25	89.37	78.93	90.295	89.58	89.74	78.12	90.344
Cosine KNN	86.16	78.83	77.87	61.22	83.585	85.74	85.97	78.23	86.083	86.19	86.42	77.51	85.901
Cubic KNN	85.89	81.69	80.02	64.39	86.328	87.41	87.73	75.37	86.050	87.84	88.04	74.48	85.767
Fine KNN	92.02	84.20	82.96	64.06	88.386	91.49	91.69	84.35	91.870	91.99	92.11	84.45	91.945
Medium Gaussian SVM	68.85	39.57	36.19	26.75	75.571	61.11	62.21	66.44	80.271	67.18	67.67	67.59	80.398
Linear SVM	22.67	23.97	25.31	22.38	59.259	22.80	22.61	23.06	59.259	22.49	22.79	23.34	59.259
Fine Gaussian SVM	71.41	54.45	52.25	44.74	85.188	71.22	71.84	66.34	83.636	70.25	72.26	64.37	83.433
Quadratic SVM	23.99	23.49	23.43	22.02	59.586	26.26	25.63	23.90	77.165	25.12	25.82	24.19	76.891
Cubic SVM	24.22	23.19	23.46	21.71	34.225	70.12	25.53	23.91	77.925	26.03	26.10	23.82	85.397
Proposed CNN	82.46	77.19	77.40	68.86	90.116	85.75	85.89	88.23	96.562	86.65	86.78	90.47	96.726

sensing matrix while maintaining competitive or superior accuracy. When compared to reconstruction-based studies like [47] or [48], our method circumvents the computational expense of inverse recovery algorithms (e.g., GPSR, BSBL), thereby enhancing scalability and deployment feasibility in edge computing scenarios.

Therefore, our proposed framework demonstrates that the integration of a fixed, structured sparse binary sensing matrix with a dedicated CNN classifier enables highly accurate ECG classification without reconstruction. It combines the interpretability and hardware-efficiency of deterministic sensing with the learning capacity of deep models making it a highly suitable solution for real-time, low-power cardiac monitoring systems.

VI. DISCUSSION

The findings of this study stress the effectiveness of the proposed compressed learning framework, which used structured sparse binary sensing matrix in conjunction with a deep CNN classifier for efficient ECG classification.

Across a broad range of compression ratios (CR = 0.1 to 0.9), the proposed system consistently achieved high classification performance. Notably, an optimal trade-off between accuracy and compression was observed at CR = 0.5, where the model achieved an accuracy of 96.56%, a specificity of 97.9%, and an F1-score of 96.5%. These metrics indicate a

well-balanced classifier, capable of both high sensitivity and precision. Even at higher compression levels (CR = 0.1), the performance remained robust, with an accuracy of 90.116% and specificity of 93.90%.

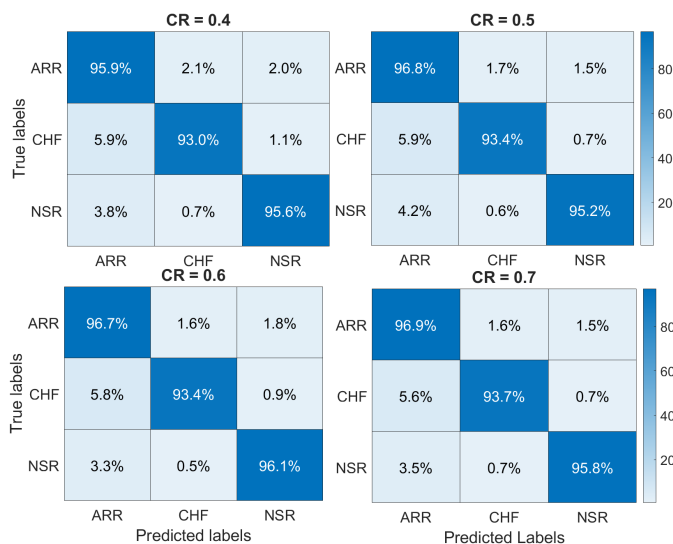


Fig. 4: Confusion Matrix at CR= 0.4-0.7

A key design advantage is the deterministic block diagonal structure of the proposed sensing matrix, which preserves

TABLE VI: Comparison with State-of-the-Art Studies

Ref.	Signal Types	Compressed Sensing Yes/No (Type)	Classification Approach	Compression Ratio	Reconstruction Approach	Accuracy (%)	Specificity (%)	F1-Score (%)
[43] 2023	ARR, CHF, NSR	Yes Deep Compressed Sensing	CNN	CR = 0.2	-	98.16	-	98.06
[40] 2025	ARR, CHF, NSR	No DCT based compression	kNN	-	-	97.00	-	-
[41] 2024	ARR, CHF, NSR	No CWT based compression	Pre-trained CNN	-	-	98.7	99	98.33
[45] 2023	ARR, CHF, NSR	Yes Optimized Walsh-Hadamard SM	CNN+original ECG CNN+compressed ECG CNN+Fully reconstructed	Not specified	SPGL1	95.00 92.82 94.89	96.44 97.44	-
[42] 2022	ARR, CHF, NSR	No	Hybrid deep CNN approach LDA classifier	10000 segment samples	-	98.74	99.00	-
[47] 2025	ARR, CHF, NSR	Yes DWT DCT	Reconstructed Signals + CWT-DCNN Reconstructed Signals + STFT-DCNN Compressed signal + STFT-DCNN	Window length = 256 CR=0.5	GPSR	98.40	—	98.378
[44] 2023	ARR (N, S, V, F, Q)	Yes Learnable SM	CSML-Net	0.1 0.3 0.5	-	97.82 97.97 98.13	-	89.09 89.53 90.18
[28] 2021	AFDB	Yes Deterministic SM	Transposed Projection - Convolutional Neural Network	-	Transpose Projection SDMM	99.32	99.43	99.14
[31] 2020	MIT-BIH Atrial Fibrillation	Yes Random Sparse SM	CS-CNN	0.5	-	94.46	94.54	94.47
[48] 2019	MIT-BIH Arrhythmia (N,A)	Yes Sparse Binary SM	Reconstructed Signals + DNN	0.2 0.7	BSBL	86.74 98.44	21.91 95.67	-
[46] 2020	MIT-BIH Atrial Fibrillation	yes, SBM, RGM	DNN	50% 60% 70%	-	95.81 95.16 94.46	96.29 95.70 94.70	96.65 96.13 95.59
Our Method	ARR, CHF, NSR	Yes Sparse Binary SM	CNN	0.5 0.6 0.7	-	96.56 96.14 96.42	97.9 97.6 97.8	96.5 96.14 96.42

locality and reduces signal distortion during compression. The strong performance at CR = 0.5 can be attributed to the uniform block allocation, which reduces inter-column correlation and preserves signal morphology. Although RIP conditions are not strictly necessary for compressed-domain inference, the structured sparsity of the proposed matrix supports stable embeddings of ECG features, ensuring that essential discriminative information is preserved for classification. This structure facilitates more effective feature extraction than unstructured alternatives such as random Gaussian or Bernoulli matrices. This synergy is reflected in the comparative results: the proposed sensing matrix outperforms Random Gaussian, Random Bernoulli, and Structured Fourier matrices by margins up to 13% in accuracy at low CRs and maintains a 7–10% advantage at higher CRs.

From a classifier perspective, the proposed CNN demonstrated superior validation accuracy compared to state-of-the-art ML classifiers. The CNN outperformed the next best performing model, the Subspace KNN Ensemble, by approximately 3% across most CRs. For example, at CR = 0.5, our CNN achieved 96.56% accuracy versus 93.57% for the Subspace KNN Ensemble. Classical ML models underperformed in part due to their reliance on handcrafted or shallow features, which are insufficient to capture the morphological complexity of compressed ECG signals.

During training, the CNN effectively explores the compressed feature space by learning invariant morphological patterns preserved by the deterministic block-sparse sensing matrix. Because the matrix maintains local temporal structure across all CRs, the training data exhibit stable feature distributions that facilitate robust feature learning. During testing, the model exploits these learned representations by utilizing the consistent compressed-domain patterns to generalize across unseen ECG segments, arrhythmia types, and compression ratios. This explains the model's high generalization performance and its stable accuracy at moderate-to-high CRs.

Evaluation using confusion matrices further validates the

discriminative power of the proposed framework. As shown in Fig. 4, at CR = 0.5 the true positive classification rates for ARR, CHF, and NSR were 96.7%, 95.9%, and 97.2% respectively. Misclassifications were minimal and uniformly distributed across classes, indicating the model generalization across diverse cardiac conditions.

Moreover, ROC curve analysis (Fig. 5) shows that the area under the curve (AUC) for all three classes ARR, CHF, and NSR was 0.99 at both CR = 0.5 and CR = 0.6. This confirms near perfect separability of the model and validates the robustness of its predictions even under increased compression. Such high AUC values imply that the classifier maintains high sensitivity without sacrificing specificity. While replacing CS with a conventional undersampling scheme would require retraining a separate model and would not constitute a methodologically equivalent comparison. Since the proposed framework is explicitly designed to operate on information-preserving CS measurements, direct substitution with undersampling falls outside the intended scope and design assumptions of the model.

Comparative analysis with state-of-the-art studies revealed that while some approaches achieve marginally higher accuracy (e.g., 98.16% in [43]), they either require full signal reconstruction, learnable sensing matrices, or involve deep encoder-decoder architectures with higher inference cost. For instance, GPSR-based frameworks such as in [47] achieve 98.4% accuracy but depend on expensive iterative reconstruction. In contrast, our method avoids reconstruction entirely and still reaches 96.56–96.73% accuracy with 97.8–97.9% specificity and over 96% F1-score, all while preserving computational simplicity and hardware-friendliness. From a clinical perspective, this framework offers a pathway toward practical wearable cardiac monitoring systems that balance diagnostic accuracy with the computational and energy constraints of ambulatory devices. Future clinical validation studies will be essential to demonstrate real-world efficacy and integration into existing care pathways.

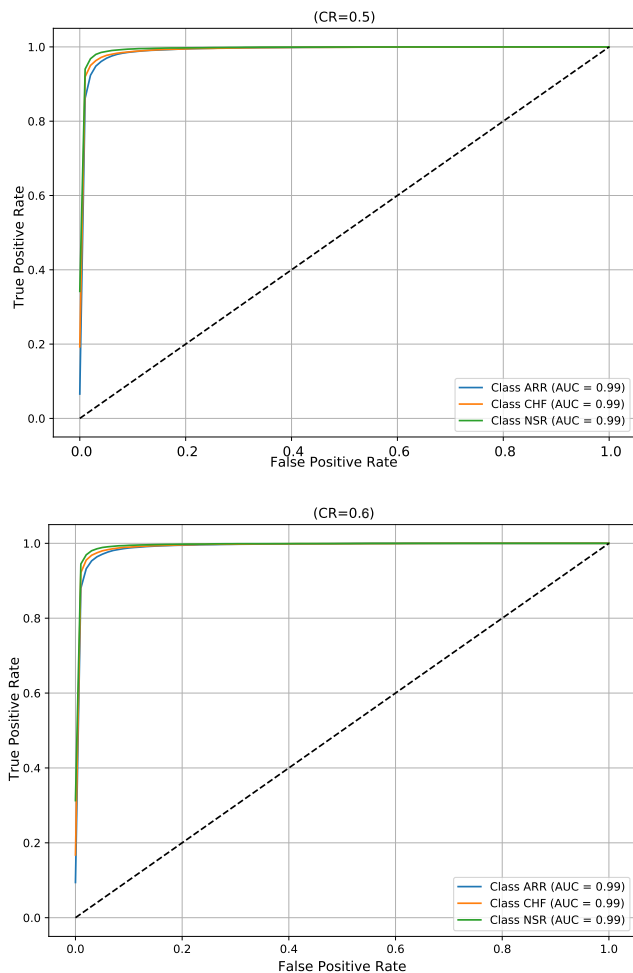


Fig. 5: ROC curves of CNN classifier at CR = 0.5 and CR = 0.6, showing classwise AUC values.

In summary, the proposed framework effectively balances classification accuracy, computational efficiency, and implementation simplicity. The combination of a deterministic, low-complexity sensing matrix and a lightweight, high-performing CNN enables real-time ECG analysis from compressed measurements.

A. Implementation on embedded system

We implemented only the ECG compression or CS encoder stage, based on the proposed sensing matrix on the STM32 NUCLEO-F401RE microcontroller operating at a clock frequency of 84 MHz. While the subsequent machine learning-based classification is performed off-device. This embedded implementation therefore focuses on validating the feasibility, efficiency, and real-time performance of the compression stage, which constitutes the most computationally constrained component in wearable ECG systems. The aim was to evaluate whether the proposed sensing matrix could meet the timing, memory, power and energy constraints imposed by edge devices and wearable health monitors. For this validation, pre-recorded ECG segments obtained from public PhysioNet datasets were used and streamed to the microcontroller to

emulate real-time signal acquisition. No live patient data acquisition was performed in this study. The structured design of the sensing matrix offers several advantages for embedded implementation. Its binary and sparse nature eliminates the need for multiplication or floating-point operations, relying solely on simple additions and memory indexing. This architectural simplicity translates directly to reduced computational complexity and consistent execution time, irrespective of the compression ratio.

In our setup, ECG signals were sampled at 128 Hz, which provides a 7.8125ms interval between samples. This defines the upper bound for processing time available to the microcontroller for each compression task. Figure 6 (a) illustrates the system block diagram of the microcontroller implementation and Fig. 6(b) shows the CS encoder execution timing diagram.

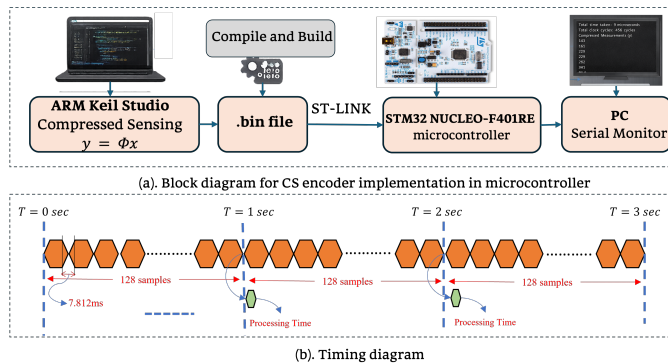


Fig. 6: (a) Hardware implementation block diagram. (b) Timing diagram for real-time CS encoder execution on microcontroller

We programmed the microcontroller using the Keil Studio Cloud platform and evaluated energy consumption using STM32CubeMX’s power estimation tools. Execution time was measured using the on-chip DWT (Data Watchpoint and Trace) cycle counter and mbed timer, while runtime statistics were transmitted to a host PC through UART and monitored using a serial terminal as shown in the Fig. 6(a).

During the compression operation, the execution time was consistently measured at 9 μs across all compression ratios, corresponding to approximately 700 clock cycles. This represents only 0.115% of the available sampling interval, leaving over 99.8% of the cycle idle. Additionally, each compression consumed approximately 0.641 μJ of energy, with an average current draw of 21.6 mA and a power consumption of 71.29mW. The compression operation required 35 KB of flash memory (out of 512 KB) and 10 KB of RAM (out of 96 KB), making it highly suitable for deployment on lightweight, resource-constrained embedded platforms.

The processing time and energy usage remained constant across all tested compression ratios. This is a direct consequence of the matrix fixed sparsity: each matrix regardless of CR contains exactly 128 non-zero elements. As a result, the computational load is invariant, allowing predictable and optimized scheduling in real-time systems. The microcontroller-based implementation demonstrates that the proposed sensing matrix not only offers theoretical compression advantages but

also translates effectively into practical, real-world embedded applications.

In examining the computational complexity of the CS encoder, each element of a random sensing matrix is stored using a fixed-point or floating-point representation requiring b bits per element (e.g., $b = 32$ or 64 bits). Accordingly, the total memory required to store a dense sensing matrix scales as $M \times N \times b$ bits, where M and N denote the matrix dimensions. The Gaussian matrix presents the highest computational complexity, as the corresponding CS encoder must execute both $M \times N$ multiplication and $M \times (N - 1)$ addition operations. The Bernoulli matrix simplifies implementation by eliminating multiplication operations, while still requiring storage of $M \times N$ binary-valued elements and the same number of addition operations. In contrast, the proposed deterministic sparse binary sensing matrix does not require explicit storage of matrix coefficients, as its structure is implicitly defined. As a result, it significantly reduces memory requirements and requires only $N - M$ addition operations during the CS compression stage, making it highly suitable for resource-constrained embedded platforms.

B. Limitations and Future Work

Despite the strong performance and practical advantages of the proposed compressed learning framework, few limitations warrant further investigation. First, although the sparse binary sensing matrix greatly simplifies hardware implementation and preserves high classification accuracy, its deterministic nature limits adaptability to varying ECG signal dynamics, patient-specific variability, and inter-device differences. Future work could explore the integration of adaptive or semi-learnable structured sensing matrices to address this limitation.

Second, this study was conducted using three benchmark PhysioNet datasets (ARR, CHF, NSR) that were recorded under controlled clinical conditions and contain relatively clean ECG signals. In contrast, wearable and ambulatory ECG systems are often subject to substantial motion artifacts, electrode impedance variability, baseline drift, and environmental noise. While the block-sparse deterministic design of our sensing matrix may inherently improve robustness by preserving local ECG morphology, explicit evaluation on noisy wearable datasets remains an essential step. Future work will investigate noise-aware data augmentation, adaptive filtering, and robust training strategies to enhance generalization to real-world settings. Future work will also include validation on additional external ECG datasets with different annotation schemes, such as publicly available Mendeley repositories [49], to further assess cross-dataset generalization.

Third, the proposed classification framework operates under a closed-set assumption and is trained to distinguish only three ECG classes (ARR, CHF, and NSR). Consequently, ECG signals corresponding to unseen cardiac conditions or out-of-distribution patterns are forced into one of the predefined classes. The current study does not incorporate an explicit out-of-distribution detection or rejection mechanism; addressing this limitation using open-set classification, confidence-based abstention, or anomaly detection techniques will be explored in future work.

Fourth, although the current model is lightweight and optimized for embedded platforms, quantization-aware training and low-power hardware acceleration (e.g., FPGA or RISC-V based deployment) have not yet been explored. These directions can significantly improve energy efficiency, enabling continuous cardiac monitoring on ultra-low-power devices.

Finally, while this work focused on three-class classification, many ECG applications require beat classification across multiple arrhythmic subtypes. Future work could extend this architecture to multi-label or hierarchical classification problems and validate on broader patient populations across demographics. In addition, scalability to longer ECG recordings and higher sampling rates should be evaluated, since these may impose higher memory and throughput demands. Furthermore, the framework will be explored on resource-constrained hardware platforms beyond microcontrollers, such as Field Programmable Gate Arrays (FPGAs) and reduced instruction set computer (RISC)-based System on Chips (SoCs), to ensure generalization across diverse deployment scenarios.

VII. CONCLUSION

In this work, we proposed a compressed learning framework for real-time ECG classification, combining a structured sparse binary sensing matrix with a lightweight CNN classifier. This architecture enables direct classification from compressed measurements, eliminating the need for computationally expensive reconstruction and achieving a balance between accuracy and efficiency. Extensive experiments demonstrated that the proposed method achieves robust classification performance across a wide range of compression ratios, with 96.56% accuracy, 97.9% specificity, and 96.5% F1-score at CR = 0.5. The confusion matrix analysis confirmed consistent classification across all classes (ARR, CHF, NSR), while ROC curves at CR = 0.5 and CR = 0.6 achieved near-perfect AUCs of 0.99 for each class highlighting the model reliability and diagnostic utility. Compared to conventional ML models and state-of-the-art studies, our method demonstrated superior accuracy without the need for signal reconstruction or complex learnable sensing matrices. The fixed binary sensing matrix offers significant hardware advantages, positioning the framework as a viable solution for low-power wearable ECG monitoring systems.

REFERENCES

- [1] B. Lal, R. Gravina, F. Spagnolo, and P. Corsonello, "Compressed sensing approach for physiological signals: A review," *IEEE Sensors Journal*, pp. 1–1, 2023.
- [2] D. L. Donoho, "Compressed sensing," *IEEE Transactions on information theory*, vol. 52, no. 4, pp. 1289–1306, 2006.
- [3] K. Kulkarni and P. Turaga, "Reconstruction-free action inference from compressive imagers," *IEEE transactions on pattern analysis and machine intelligence*, vol. 38, no. 4, pp. 772–784, 2015.
- [4] S. Lohit, K. Kulkarni, P. Turaga, J. Wang, and A. C. Sankaranarayanan, "Reconstruction-free inference on compressive measurements," in *Proceedings of the IEEE conference on computer vision and pattern recognition workshops*, 2015, pp. 16–24.
- [5] X. Bian, W. Xu, Y. Wang, L. Lu, and S. Wang, "Direct feature extraction and diagnosis of ecg signal in the compressed domain," *IEEE Sensors Journal*, vol. 21, no. 15, pp. 17 096–17 106, 2021.
- [6] W. Li, H. Chu, B. Huang, Y. Huan, L. Zheng, and Z. Zou, "Enabling on-device classification of ecg with compressed learning for health iot," *Microelectronics Journal*, vol. 115, p. 105188, 2021.

- [7] M. M. Abo-Zahhad, A. I. Hussein, A. M. Mohamed *et al.*, "Compression of ECG signal based on compressive sensing and the extraction of significant features," *International Journal of Communications, Network and System Sciences*, vol. 8, no. 05, p. 97, 2015.
- [8] T.-W. Sun, D. Ali, and A. Wu, "Compressed-domain ecg-based biometric user identification using task-driven dictionary learning," *ACM Transactions on Computing for Healthcare (HEALTH)*, vol. 3, no. 3, pp. 1–15, 2022.
- [9] B. Lal, Q. Li, R. Gravina, and P. Corsonello, "ECG signals analysis based on compressed sensing and learning techniques for heart disease recognition," in *2023 7th International Multi-Topic ICT Conference (IMTIC)*, 2023, pp. 1–7.
- [10] Z. Zhang, T.-P. Jung, S. Makeig, and B. D. Rao, "Compressed sensing for energy-efficient wireless telemonitoring of noninvasive fetal ECG via block sparse bayesian learning," *IEEE Trans. Biomed. Eng.*, vol. 60, pp. 300–309, 2013.
- [11] V. Izadi, P. K. Shahri, and H. Ahani, "A compressed-sensing-based compressor for ECG," *Biomed. Eng. Lett.*, vol. 10, pp. 299–307, 2020.
- [12] S. Abhishek, S. Veni, and K. Narayanankutty, "Biorthogonal wavelet filters for compressed sensing ECG reconstruction," *Biomed. Signal Process. Control*, vol. 47, pp. 183–195, 2019.
- [13] Z. Zhang, X. Liu, S. Wei *et al.*, "Electrocardiogram reconstruction based on compressed sensing," *IEEE Access*, vol. 7, pp. 37228–37237, 2019.
- [14] M. Melek and A. Khattab, "ECG compression using wavelet-based compressed sensing with prior support information," *Biomed. Signal Process. Control*, vol. 68, p. 102786, 2021.
- [15] J. A. Jahanshahi, H. Danyali, and M. S. Helfroush, "Compressive sensing based multi-channel ECG reconstruction in wireless body sensor networks," *Biomed. Signal Process. Control*, vol. 61, p. 102047, 2020.
- [16] J. Saliga, I. Andr as, P. Dolinsk y *et al.*, "ECG compressed sensing method with high compression ratio and dynamic model reconstruction," *Measurement*, vol. 183, p. 109803, 2021.
- [17] T. Y. Rezaei, S. Beheshti, M. Shamsi *et al.*, "ECG signal compression and denoising via optimum sparsity order selection in compressed sensing framework," *Biomed. Signal Process. Control*, vol. 41, pp. 161–171, 2018.
- [18] C. Yang, P. Pan, and Q. Ding, "Image encryption scheme based on mixed chaotic bernoulli measurement matrix block compressive sensing," *Entropy*, vol. 24, p. 273, 2022.
- [19] L. F. Polania and R. I. Plaza, "Compressed sensing ECG using restricted boltzmann machines," *Biomed. Signal Process. Control*, vol. 45, pp. 237–245, 2018.
- [20] P. R. Muduli, R. R. Gunukula, and A. Mukherjee, "A deep learning approach to fetal-ECG signal reconstruction," in *Proceedings of the Twenty Second National Conference on Communication (NCC)*, Guwahati, India, 2016, pp. 1–6.
- [21] M. Mangia, L. Prono, A. Marchioni *et al.*, "Deep neural oracles for short-window optimized compressed sensing of biosignals," *IEEE Trans. Biomed. Circuits Syst.*, vol. 14, pp. 545–557, 2020.
- [22] R. R. Shrivastwa, V. Pudi, C. Duo *et al.*, "A brain-computer interface framework based on compressive sensing and deep learning," *IEEE Consum. Electr. Mag.*, vol. 9, pp. 90–96, 2020.
- [23] M. Mangia, A. Marchioni, L. Prono *et al.*, "Low-power ECG acquisition by compressed sensing with deep neural oracles," in *Proceedings of the 2nd IEEE International Conference on Artificial Intelligence Circuits and Systems (AICAS)*, Genova, Italy, 2020, pp. 158–162.
- [24] R. R. Shrivastwa, V. Pudi, and A. Chattopadhyay, "An fpga-based brain computer interfacing using compressive sensing and machine learning," in *Proceedings of the IEEE Computer Society Annual Symposium on VLSI (ISVLSI)*, Hong Kong, China, 2018, pp. 726–731.
- [25] M. Abdelazez, F. F. Firouzeh, S. Rajan, and A. D. C. Chan, "Multi-stage detection of atrial fibrillation in compressively sensed electrocardiogram," in *2020 IEEE International Instrumentation and Measurement Technology Conference (I2MTC)*, 2020, pp. 1–6.
- [26] B. Lal, Q. Li, P. Corsonello, and R. Gravina, "Abnormal ECG detection in wearable devices using compressed learning," in *2023 IEEE International Conference on Networking, Sensing and Control (ICNSC)*, vol. 1, 2023, pp. 1–6.
- [27] G. Da Poian, C. Liu, R. Bernardini, R. Rinaldo, and G. D. Clifford, "Atrial fibrillation detection on compressed sensed ECG," *Physiological measurement*, vol. 38, no. 7, p. 1405, 2017.
- [28] H. Zhang, Z. Dong, M. Sun, H. Gu, and Z. Wang, "TP-CNN: A detection method for atrial fibrillation based on transposed projection signals with compressed sensed ECG," *Computer Methods and Programs in Biomedicine*, vol. 210, p. 106358, 2021.
- [29] A. Siddique, O. Hasan, F. Khalid, and M. Shafique, "Approxcs: near-sensor approximate compressed sensing for IoT-healthcare systems," *arXiv preprint arXiv:1811.07330*, 2018.
- [30] G. Laudato, R. Oliveto, S. Scalabrino, A. R. Colavita, L. De Vito, F. Picariello, and I. Tudosa, "Identification of r-peak occurrences in compressed ECG signals," in *2020 IEEE International Symposium on Medical Measurements and Applications (MeMeA)*, 2020, pp. 1–6.
- [31] H. Zhang, Z. Dong, J. Gao, P. Lu, and Z. Wang, "Automatic screening method for atrial fibrillation based on lossy compression of the electrocardiogram signal," *Physiological measurement*, vol. 41, no. 7, p. 075005, 2020.
- [32] Y. Arjoun, N. Kaabouch, H. El Ghazi, and A. Tamtaoui, "A performance comparison of measurement matrices in compressive sensing," *International Journal of Communication Systems*, vol. 31, no. 10, p. e3576, 2018.
- [33] S. S. Kumar and P. Ramachandran, "Review on compressive sensing algorithms for ECG signal for IoT based deep learning framework," *Applied Sciences*, vol. 12, no. 16, p. 8368, 2022.
- [34] B. Lal, R. Gravina, F. Spagnolo, and P. Corsonello, "Compressed sensing approach for physiological signals: A review," *IEEE Sensors Journal*, 2023.
- [35] A. L. Goldberger, L. A. Amaral, L. Glass, J. M. Hausdorff, P. C. Ivanov, R. G. Mark, J. E. Mietus, G. B. Moody, C.-K. Peng, and H. E. Stanley, "Physiobank, physiotoolkit, and physionet: components of a new research resource for complex physiologic signals," *circulation*, vol. 101, no. 23, pp. e215–e220, 2000.
- [36] D. S. Baim, W. S. Colucci, E. S. Monrad, H. S. Smith, R. F. Wright, A. Lanoue, D. F. Gauthier, B. J. Ransil, W. Grossman, and E. Braunwald, "Survival of patients with severe congestive heart failure treated with oral milrinone," *Journal of the American College of Cardiology*, vol. 7, no. 3, pp. 661–670, 1986.
- [37] G. B. Moody and R. G. Mark, "The impact of the mit-bih arrhythmia database," *IEEE engineering in medicine and biology magazine*, vol. 20, no. 3, pp. 45–50, 2001.
- [38] V. Abolghasemi, S. Ferdowsi, and S. Saneii, "A gradient-based alternating minimization approach for optimization of the measurement matrix in compressive sensing," *Signal Processing*, vol. 92, no. 4, pp. 999–1009, 2012.
- [39] C.-Y. Chou, Y.-W. Pua, T.-W. Sun, and A.-Y. Wu, "Compressed-domain ecg-based biometric user identification using compressive analysis," *Sensors*, vol. 20, no. 11, p. 3279, 2020.
- [40] S. Lahmiri and S. Bekiros, "An effective and fast model for characterization of cardiac arrhythmia and congestive heart failure," *Diagnostics*, vol. 15, no. 7, p. 849, 2025.
- [41] P. N. Malleswari, V. k. Odugu, T. S. Rao, and T. Aswini, "Deep learning-assisted arrhythmia classification using 2-d ECG spectrograms," *EURASIP Journal on Advances in Signal Processing*, vol. 2024, no. 1, p. 104, 2024.
- [42] A. S. Eltrass, M. B. Tayel, and A. I. Ammar, "Automated ECG multi-class classification system based on combining deep learning features with hrv and ECG measures," *Neural Computing and Applications*, vol. 34, no. 11, pp. 8755–8775, 2022.
- [43] J. Hua, B. Chu, J. Zou, and J. Jia, "Ecg signal classification in wearable devices based on compressed domain," *Plos one*, vol. 18, no. 4, p. e0284008, 2023.
- [44] S. Tang and Z. Deng, "Cs-based multi-task learning network for arrhythmia reconstruction and classification using ECG signals," *Physiological Measurement*, vol. 44, no. 7, p. 075001, 2023.
- [45] H. M. Emarar, W. El-Shafai, A. D. Algarni, N. F. Soliman, and F. E. Abd El-Samie, "A hybrid compressive sensing and classification approach for dynamic storage management of vital biomedical signals," *IEEE Access*, vol. 11, pp. 108126–108151, 2023.
- [46] Y. Cheng, Y. Hu, M. Hou, T. Pan, W. He, and Y. Ye, "Atrial fibrillation detection directly from compressed ECG with the prior of measurement matrix," *Information*, vol. 11, no. 9, p. 436, 2020.
- [47] S. S. Kumar and P. Ramachandran, "A gprs-based sparse ECG signal recovery approach for hybrid compressive sensing framework and its classification using deep convolution neural network," *IEEE Access*, vol. 13, pp. 66505–66528, 2025.
- [48] J. Hua, J. Tang, J. Liu, F. Yang, and W. Zhu, "A novel ECG heartbeat classification approach based on compressive sensing in wearable health monitoring system," in *2019 International Conference on Internet of Things (IThings) and IEEE Green Computing and Communications (GreenCom) and IEEE Cyber, Physical and Social Computing (CPSCom) and IEEE Smart Data (SmartData)*. IEEE, 2019, pp. 581–586.
- [49] P. Plawiak, "Ecg signals (1000 fragments)," *Mendeley Data*, vol. 3, p. 2017, 2017.

APPENDIX

TABLE VII: Summary of baseline models and key hyperparameters/settings

Model name (paper)	Key hyperparameters / settings
Gaussian Naive Bayes	Default parameters: var_smoothing = 1e-9; baseline generative classifier.
Kernel Naive Bayes (standardized)	Gaussian NB with default parameters applied to standardized features.
Linear Discriminant Analysis	solver = svd; multiclass linear discriminant with full covariance.
Quadratic Discriminant Analysis	Default parameters with class-specific covariance matrices.
Coarse Decision Tree	criterion = gini; max_depth = 3; max_leaf_nodes = 4; random_state = 42.
Medium Decision Tree	criterion = gini; max_depth = 4; max_leaf_nodes = 15; random_state = 42.
Fine Decision Tree	criterion = gini; max_depth = 7; max_leaf_nodes = 79; random_state = 42.
Efficient Logistic Regression	solver = lbfgs; multi_class = ovr; max_iter = 1000; tol = 1e-4; C = 1.0.
Efficient Linear SVM	Linear hinge loss; multi_class = ovr; C = 1.0; max_iter = 1000; tol = 1e-4.
Narrow Neural Network	Single hidden layer (10 units); activation = relu; alpha = 0; max_iter = 1000; random_state = 42; solver = adam.
Medium Neural Network	Single hidden layer (25 units); activation = relu; alpha = 0; max_iter = 1000; random_state = 42; solver = adam.
Bilayer Neural Network	Two hidden layers (10 units each); activation = relu; alpha = 0; max_iter = 1000; random_state = 42; solver = adam.
Trilayer Neural Network	Three hidden layers (10 units each); activation = relu; alpha = 0; max_iter = 1000; random_state = 42; solver = adam.
Wide Neural Network	Single wide hidden layer (100 units); activation = relu; alpha = 0; max_iter = 1000; random_state = 42; solver = adam.
Boosted Trees (AdaBoost)	Base estimator: max_leaf_nodes = 21; n_estimators = 30; learning_rate = 0.1; algorithm = SAMME; random_state = 42.
Kernel Logistic Regression	n_components = 100, random_state = 42; LogisticRegression: solver = lbfgs, max_iter = 1000, C = 1.0, multi_class = ovr.
Bagged Trees	Base estimator: DecisionTree (default); n_estimators = 30; max_samples = 1.0; max_features = 1.0; random_state = 42.
RUSBoosted Trees	Base estimator: DecisionTree(max_leaf_nodes = 21); n_estimators = 30; learning_rate = 0.1; random_state = 42.
Coarse Gaussian SVM	kernel = rbf; gamma = 1/64; C = 1.0; decision_function_shape = ovo; max_iter = 1000; random_state = 42.
Kernel SVM	n_components = 100, random_state = 42; SVC: C = 1.0, decision_function_shape = ovo; max_iter = 1000.
Coarse KNN	n_neighbors = 100; metric = euclidean; weights = uniform.
Medium KNN	n_neighbors = 10; metric = euclidean; weights = uniform.
Weighted KNN	n_neighbors = 10; metric = euclidean; weights = distance.
Cosine KNN	n_neighbors = 10; metric = cosine; weights = uniform.
Cubic KNN	n_neighbors = 10; metric = minkowski; p = 3; weights = uniform; n_jobs = 1.
Fine KNN	n_neighbors = 1; metric = euclidean; weights = uniform; n_jobs = 1.
Medium Gaussian SVM	kernel = rbf; gamma = 1/16; C = 1.0; decision_function_shape = ovo; max_iter = 1000; random_state = 42.
Linear SVM (kernel SVC)	kernel = linear; C = 1.0; decision_function_shape = ovo; max_iter = 1000; random_state = 42.
Fine Gaussian SVM	kernel = rbf; gamma = 1/4; C = 1.0; decision_function_shape = ovo; max_iter = 1000; random_state = 42.
Quadratic SVM	kernel = poly; degree = 2; coef0 = 1; C = 1.0; decision_function_shape = ovo; max_iter = 1000; random_state = 42.
Cubic SVM	kernel = poly; degree = 3; coef0 = 1; C = 1.0; decision_function_shape = ovo; max_iter = 1000; random_state = 42.